Analyzing hydrogen with nuclear reactions

Nuclear-reaction techniques for determining depth profiles of hydrogen, deuterium and tritium are of value in solar-cell manufacture and metallurgical problems such as steel embrittlement and radiation damage.

Samuel T. Picraux

There are many ways in which hydrogen plays an important role in today's materials problems. Our newly developed ability to detect and probe sensitively and quantitatively for hydrogen has provided valuable new insight into many of these problems. By means of nuclear-reaction techniques we can develop depth profiles of the hydrogen, deuterium and tritium concentration in various materials; these techniques have already been of practical assistance in several areas of technology, and promise to be helpful in others as well (see box on page 45). Here we shall describe rather briefly the types of nuclear-reaction techniques now used to probe for hydrogen. Then we shall concentrate on the way these techniques have been applied to studies of hydrogen isotopes in various materials, making particular note of the uses of implantation for these studies and the effect of changing the implanted-hydrogen concentration on the observed properties of the bulk materials.

Nuclear-reaction techniques

The use of ion beams to study hydrogen by nuclear-reaction techniques began around 1970 and has grown rapidly in the last couple of years.[1,2] These techniques, all of which have been demonstrated, are conveniently divided into four categories (see the table on page 47). Two of these techniques—the resonant and nonresonant reaction methods—can be considered simply as turning around the many strong nuclear reactions for protons, deuterons and tritons incident on heavier nuclei. Here the heavier nuclei are accelerated into a solid containing the hydrogen isotope.

In the first method, a resonant reaction signal arises from a given depth within the solid, a depth determined by the incident energy of the ion beam, the rate of energy loss of the ions in the solid and the energy of the resonance. If the incident ion energy is raised in steps, then at each step the resonance occurs deeper within the solid, and a depth profile of the hydrogen concentration can be built up.

The resonant reaction category consists primarily of (p,γ) resonances, which are particularly good for depth profiling.[3] The $H^1(N^{15},\alpha\gamma)$, $H^1(F^{19},\alpha\gamma)$, $H^1(B^{11},\alpha)$ and $H^1(Li^7,\gamma)$ reactions have been used, with the best depth resolution (about 40 Å near the surface) given by N^{15}, due to its narrow resonance width, and the best sensitivity (less than or equal to 10 ppm) demonstrated by Li^7, which has a wide resonance width.

The nonresonant reactions typically give better sensitivity within a thick layer. By energy analysis of the emitted products, this method can also be used for less sensitive depth profiling, and depth profiling has been demonstrated for $H^2(He^3,\alpha)$, $H^2(d,p)$, $H^2(d,n)$, $H^3(p,n)$ and $H^1(t,n)$.

Elastic scattering of protons from deuterium and tritium can be made sufficiently sensitive over scattering from other elements in the target by taking advantage of the preferentially enhanced nuclear-scattering cross sections at large angles and at energies of 2 to 3 MeV (about 10^2 to 10^3 times the Rutherford cross section). The relative sensitivity is further improved by using thin targets (usually less than 10 microns). Although the final hydrogen sensitivity is low for elastic scattering (typically about one atomic percent), this method is quite versatile since the concentration of all other heavier elements in the samples is obtained at the same time. For thin targets elastic recoil methods are useful. These methods include the detection of the recoiled hydrogen for heavy ion beams or the coincidence detection of both the incident and recoiled particles for incident hydrogen, and they can have very high sensitivity as well as give the depth profile.

The major advantages of nuclear-reaction techniques is that the detected interaction is independent of matric composition and that the cross sections, once measured, permit the determination of absolute quantities by these measurements.

The ability of nuclear techniques to determine depth profiles is extremely valuable in solid-state studies. The *absolute* depth scale is dependent on the elemental composition of the target, which can be accurately determined independently by ion backscattering (see the article by James Ziegler in PHYSICS TODAY, November 1976, page 52) or other means. The effect of each element can then be included reasonably accurately by additivity rules. The fundamental unit of depth measured is atoms per cm^2, and this measurement can be converted into depth in centimeters, provided that the density is known. These measurements are almost nondestructive, although some radiation damage is induced by the ion beam. The energy-loss rates of ion beams restrict measurements to the near surface region of solids: Typical maximum probing depths range from 1 to 10 microns, depth resolutions from 50 Å to 1000 Å and sensitivities from 10^{-2} to 10^{-5} (all hydrogen fractions here are atomic) for hydrogen isotopes.

Hydrogen implant studies

The application of nuclear-reaction methods to studies of implanted hydrogen has important implications, primarily for reactor technology. In these studies, we use ion beams in two ways: to implant the hydrogen and then to analyze its be-

Samuel T. Picraux is supervisor of the Ion-Solid Interactions Research Division at Sandia Laboratories, Albuquerque.

havior. Advantages of the ion-beam techniques for implantation are that at sufficiently low temperatures, the hydrogen concentration and depth distribution can be controlled independently of thermodynamic constraints, as we shall see. Then nuclear-reaction analysis can provide sensitive absolute detection and depth profiles. In addition, ion-channeling techniques can determine such crystallographic information as the location of the hydrogen, on the various sites available to it within the crystal lattice, or the depth distributions of disorder.

In studying implanted hydrogen, several regimes of behavior are found as the hydrogen concentration is increased. The dilute phase is taken to be the situation in which the hydrogen is surrounded by a perfect crystal lattice. At temperatures where the hydrogen becomes mobile, it may find and interact with imperfections such as defects or impurities in the lattice and in some cases become trapped. At higher concentrations precipitation either as a hydride phase or as hydrogen gas bubbles will occur. At extremely high concentration, for the case where gas bubbles are believed to form, sufficient stresses can occur so that surface deformations, such as blistering, can occur.

In figure 2 we see an illustration of the nonresonant reaction method for detecting deuterium by means of a He^3 analysis beam. The high exothermicity (Q is about 18 MeV) and large cross section (about 70 millibarns per steradian) of the reaction are of particular advantage here

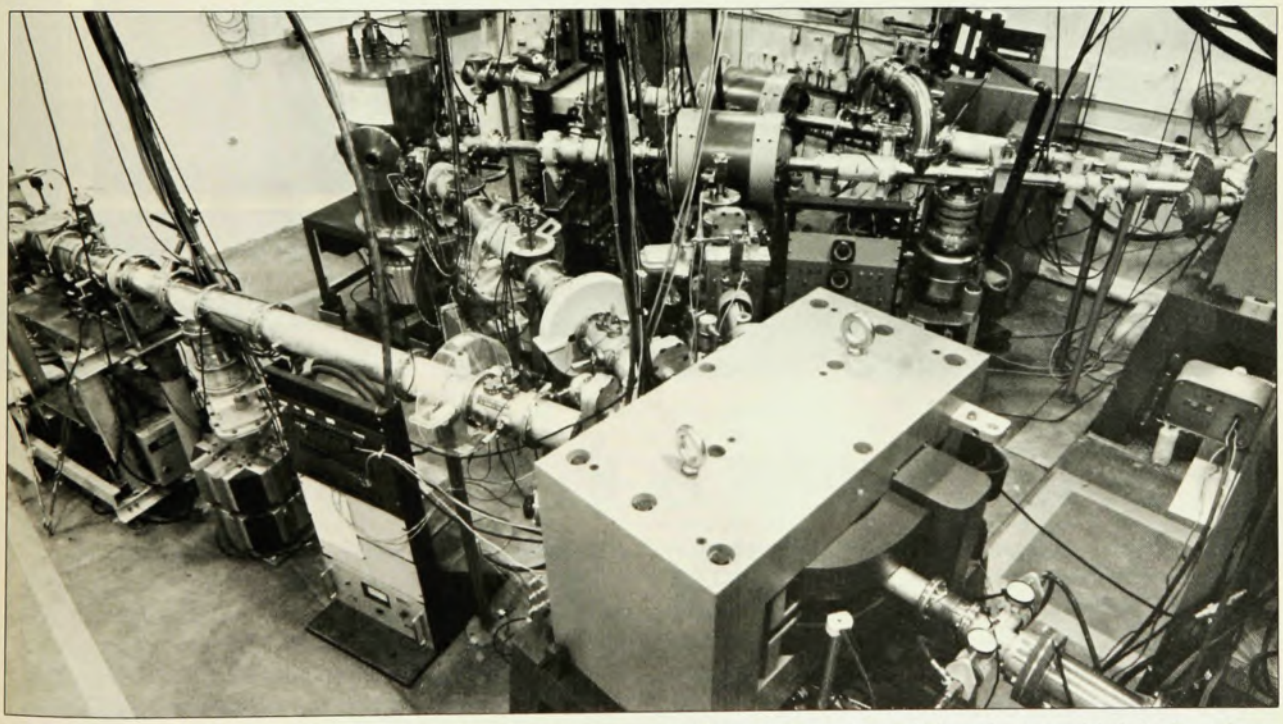

Studies of hydrogen isotope implantation and nuclear-reaction analysis are carried out at Sandia Laboratories in Albuquerque, New Mexico. The photograph shows beam lines and analyzing magnets from two accelerators; entering at bottom right is the beam from a 2 MW Van de Graaff, used for nuclear-reaction analysis, and at upper right is the beam from a 0–400 kV accelerator, used for hydrogen implantation. The chamber at rear left—where two beam lines intersect—is the location of the *in situ* studies described in this article. Figure 1

The Computer for the Professional

Whether you are a manager, scientist, educator, lawyer, accountant or medical professional, the System 8813 will make you more productive in your profession. It can keep track of your receivables, project future sales, evaluate investment opportunities, or collect data in the laboratory.

Use the System 8813 to develop reports, analyze and store lists and schedules, or to teach others about computers. It is easily used by novices and experts alike.

Reliable hardware and sophisticated software make this system a useful tool. Several software packages are included with the machine: an advanced disk operating system supporting a powerful BASIC language interpreter, easy to use text editor, assembler and other system utilities. Prices for complete systems start at $3250.

See it at your local computer store or contact us at 460 Ward Dr., Santa Barbara, CA 93111, (805) 967-0468.

PolyMorphic Systems

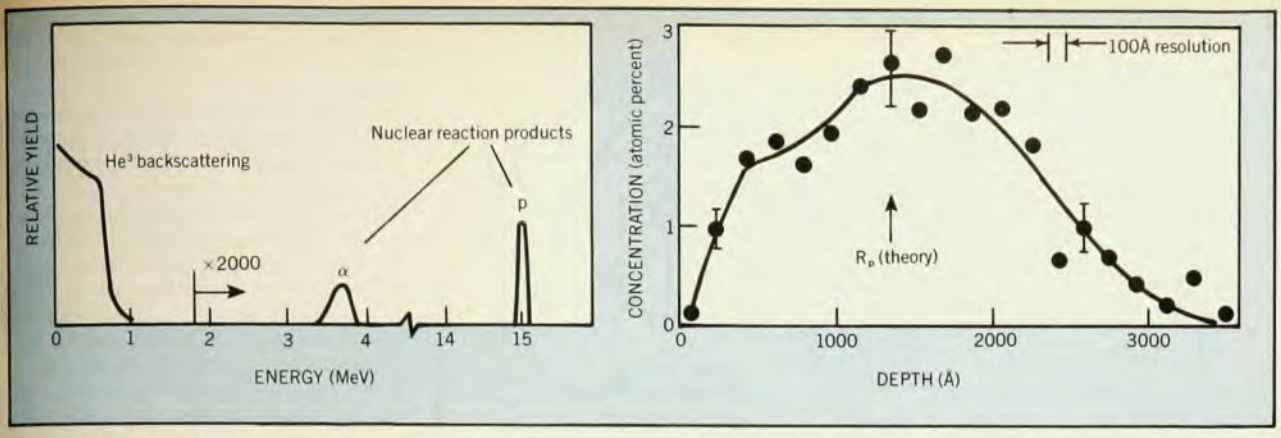

Depth profile for deuterium in tungsten is determined with a nonresonant technique. When a 750-keV He^3 beam is directed at a W target containing H^2, the reaction H^2 (He^3, α)H^1 occurs. The intensity of the alpha-particle signal at a given detected energy and angle (left) is a measure of the H^2 concentration at a given depth. By energy analyzing the emitted alpha particles, a depth profile (right) for H^2 implanted as a 32-keV beam in W can be obtained. Depth resolution is about 100 Å, and the profile has a characteristic maximum near the projected range R_p. Distortion from the Gaussian shape near the surface may be a result of hydrogen trapping. Figure 2

and give a high sensitivity for deuterium detection: Far less than a monolayer of deuterium in the near surface of a solid is quite readily detectable. This high sensitivity comes about because in such a positive Q reaction, the alpha particle and proton are emitted at high energies on a very low noise background. We can also obtain the depth distribution of the deuterium by energy analysis of the emitted alpha particles. The energy-versus-depth scale arises from the ion-energy losses, primarily to electronic excitations, as the incident and emitted particles pass through the solid. These losses are superimposed upon the energy change resulting from the nuclear interaction. At a laboratory angle of 77 deg the detected alpha particles will all be created at the same energy, even though the 750-keV He^3 analysis ions that induce the reaction are losing energy with increasing depth. For this particular angle and reaction, then, the depth scale is almost exactly given by the energy loss of the emitted alpha particles to electronic excitations as the alpha particles travel out of the sample. An example of the depth profile at a level of several atomic percent for a deuterium-implanted tungsten crystal (about 3×10^{16} deuterium atoms per cm^2) is seen on the right side of figure 2. The depth resolution achieved for a glancing-angle detection of 10 deg with the surface is about 100 Å. The profile has a characteristic maximum around the predicted range, and there is some distortion from a Gaussian profile near the surface, possibly related to trapping of hydrogen at ion-induced radiation damage sites.

Crystal-site determination

Crystallographic information, such as the type of lattice sites at which the hydrogen isotopes are located, can be obtained by lattice "channeling" of the ion beam.[4] With channeling, analysis is possible down to about an order of magnitude lower hydrogen concentrations (0.1%) than are required for neutron-scattering studies. The channeling-effect measurements require a microscopically uniform beam of ions, incident on a single crystal along low-index axes and planes. During channeling the spatial probability density of the particles does not remain uniform once inside the crystal, because the channeled particles undergo a series of correlated coulombic collisions with the atom rows or planes, taking on oscillatory trajectories. Thus, the channeled ions have a high probability density in the channel center (enhanced two or three times) and a very low probability density within a screening distance of the rows (reduced 20 to 50 times). This redistribution in the spatial density of the particles means that an interstitial impurity will have a much higher interaction yield than a substitutional impurity. Detailed angular scans give information on the projected crystallographic position of the impurity. Then measurements along

Why study hydrogen?

The relatively simple techniques discussed here for detecting hydrogen isotopes and determining their depth profiles have, as we have noted, expanded rather rapidly in just the past few years. At least part of the motivation for this growth is the wide variety of practical materials problems, particularly in relation to energy, to which these techniques are now being applied.

Microelectronics. There is general interest in the role of hydrogen in the properties of films. Of particular interest is the possibility of doping amorphous semiconductors for solar-cell applications. The addition of hydrogen to these materials ties up the dangling bonds, removing the mid-gap states; the amorphous silicon layers can then be doped to form both n-and p-type semiconductors. With this control it has been possible to make amorphous solar cells with efficiencies in excess of 5%. Hydrogen profiles have already been analyzed by nuclear-reaction techniques in such materials.[15]

In semiconductor memory devices made of metal and nitride oxide (MNOS devices), the charge-storage mechanism in the nitride layer is not yet understood. However, there is evidence that the high hydrogen concentration plays an important role here.

Fossil energy. Hydrogen embrittlement has long been a concern of major economic significance in metallurgy. This embrittlement will become an increasingly important problem with the possible advent of a hydrogen economy. For example, failure in certain high-strength steels has been attributed to hydrogen embrittlement initiated by high hydrogen concentrations in electroplated coatings such as cadmium or chromium, and such coatings have been analyzed for hydrogen by nuclear reactions.[16]

Reactor technology. Certain types of radiation damage, such as energetic-ion damage, create extremely deep traps for hydrogen in certain materials.[6] In a fusion reactor this could have very serious consequences for radioactive-tritium inventory considerations. Fortunately this effect does not appear to be so large in the stainless steels.

Very recently, high hydrogen concentrations have been found by reaction techniques in certain superconducting Nb_3Ge films, and the increased concentration has been correlated with reduced superconducting transition temperatures.[17] In nuclear physics, ion-beam studies have attempted to determine whether or not surface concentrations of hydrogen present on materials used for neutron bottles can explain their low storage efficiencies for ultracold neutrons, relative to theoretical predictions.[18]

Catalysis. Although the surface structure of hydrogenation catalysts have not yet involved nuclear reaction techniques, work in this area is anticipated.

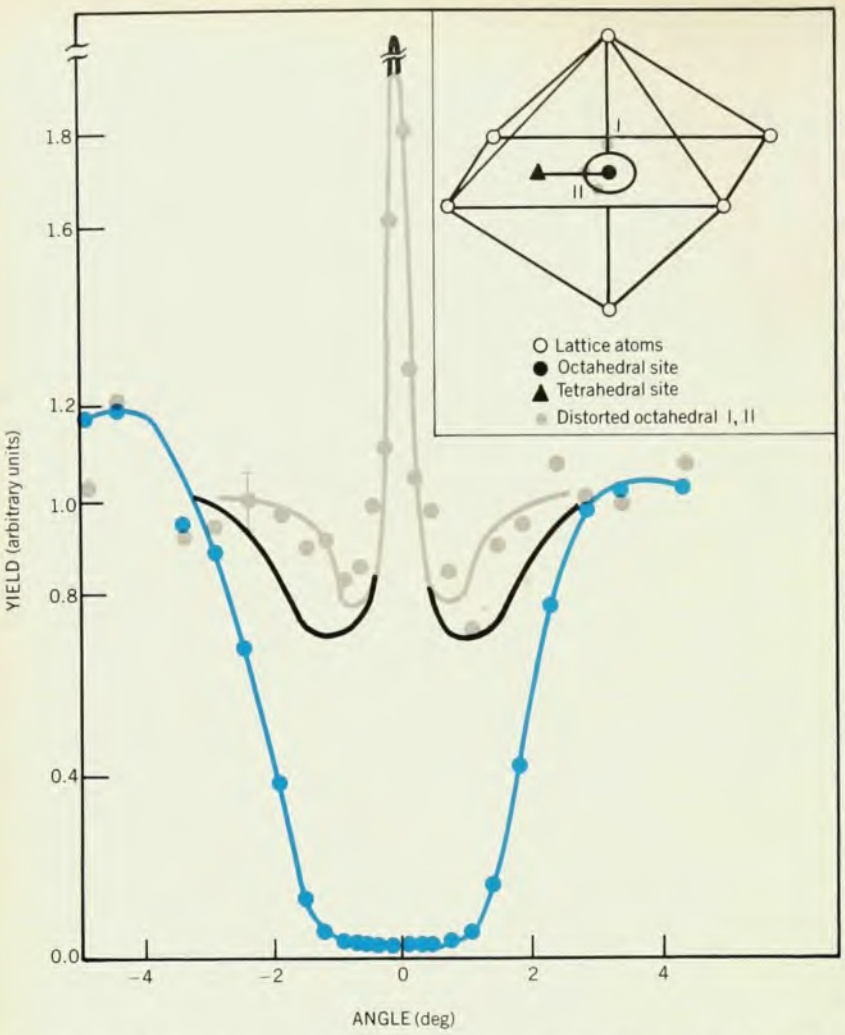

Channeling analysis of deuterium implanted in molybdenum. After the H^2 is implanted, the sample is annealed to 296 K. Analysis is accomplished with the $H^2(He^3, \alpha)H^1$ reaction, induced by a 700-keV He^3 beam, which also backscatters from the Mo. A plot of signal intensity as a function of sample tilt angle for the beam incident along the ⟨100⟩ crystal axis shows a peak for the H^2 (gray circles) and a dip for the Mo (colored circles), indicating that the H^2 impurity occupies an interstitial site. The calculation for a distortion of about 0.2 Å about the octahedral interstitial site (gray) agrees more closely with experiment than the calculation for a simple octahedral interstitial site (black) (see inset). From reference 5. Figure 3

other directions determine the impurity site in three dimensions. Comparisons with calculations are usually required for nonsubstitutional site interpretation.

The channeling technique for impurity location is fairly straightforward to apply, although some skill is required for interpretation. In figure 3 is an illustration of a ⟨100⟩-axis analysis for implanted deuterium in molybdenum, to indicate the sensitivity of the technique for well defined interstitial positions.[5] In this angular scan of the crystal orientation about the ⟨100⟩ direction, the signal from the implanted deuterium, resulting from the $H^2(He^3,p)He^4$ reaction, is simultaneous with the elastic-scattering signal from the lattice atoms at corresponding depths. A substitutional H^2 impurity would give a dip coincident with that for the lattice atoms, whereas the observed sharp "flux peak" is characteristic of an impurity in the central region of the channel; that is, an interstitial impurity. Further analysis along other directions shows that the deuterium is located in a distorted position near the octahedral interstitial site. The gray and black lines are the calculated angular yield distributions for two different sites. The gray line, which corresponds to the deuterium being distorted about 0.2 Å from the octahedral interstitial site and in the shaded plane normal to the direction of the nearest neighbor positions, gives much better agreement with the data than the calculated yield for the simple octahedral interstitial location. This case is quite favorable, in that a distortion of only 0.2 Å from the pure octahedral site can be distinguished.

This example comes from a series of implantation studies of dilute deuterium locations in the group VI transition metals at 90 K and for trapped sites upon annealing to 296 K. The results of the measurements at 90 K indicate that, for chromium and molybdenum but not for tungsten, a change of site from tetrahedral to octahedral can take place when the deuterium becomes mobile.

The predominantly tetrahedral location for low-temperature implants in Cr, Mo and W is not unexpected theoretically for the body-centered cubic metals. This observation appears consistent with the interpretation that at sufficiently low temperatures, where the deuterium is immobile, the dilute phase of a system may be studied by these ion-beam techniques, even though the thermodynamic solid solubility is exceeded locally. However, upon annealing to temperatures where the deuterium can move, we find subsequent trapping with the deuterium remaining bound until much higher temperatures. These unusual trap sites are very specific and invoke speculation on the nature of the trap center.

At concentrations of a few tenths percent D, more than one deuterium could be involved in the center, due to D–D interactions. Alternatively, defects such as vacancies, which were introduced during the 15-keV implantations, could be associated with the center. Either of these possibilities could account for the lowered symmetry, and they cannot be directly distinguished from each other by channeling because only the impurity position and not the surrounding distortions can be determined. There is, however, a way to examine the mechanism of trapping. We can compare the trapping efficiencies for molecular D_3^+ and monatomic D_1^+ implants at low concentrations for corresponding energies per D atom. Although the D_3^+ molecule breaks up upon entering the solid, the constituent D atoms will still have a final mean distance much nearer to each other than for monatomic implants at low concentrations (about 0.01%). This difference should allow hydrogen–hydrogen and hydrogen-defect trapping mechanisms to be distinguished, and preliminary studies for tungsten suggest a defect trapping mechanism.

Damage trapping of hydrogen

Hydrogen-damage trapping effects can be examined in more detail by introducing the damage separately from the hydrogen. For such studies it is very valuable to have a depth profile, and good use is made of the sensitive resonant-reaction technique. One example is the 16.4-MeV F^{19} resonance with H^1. Here the emitted gamma rays are detected with a near-surface depth resolution of about 200 Å, and energy straggling causes a broadening of this resolution with increasing depth. Typically there is a large hydrogen signal from the surface when working with H^1, the naturally abundant isotope. Thus, sensitivity may be limited very near the surface. Surface hydrogen can come from

such phenomena as beam-induced cracking of hydrocarbons in the vacuum onto the surface or simply from the natural affinity of surfaces for hydrogen.

Two examples of trapped hydrogen profiles in molybdenum[6] are seen in figure 4. The damage was introduced by helium ions and then large amounts of hydrogen were injected, with the sample at room temperature in each case. The hydrogen is found to decorate the damage with nearly 100% retention until saturation of the enhancement in trapping, whereas without predamage a large fraction of the hydrogen is lost. The shape of the depth profile depends on the damaging ion. Enhanced trapping occurs in molybdenum not only for helium but also for a variety of chemically different ions. The trapping therefore appears to be a damage effect, not a chemical effect. Many hydrogen atoms can be trapped per implanted damaging ion. As the number of damaging ions is increased, the amount of trapping increases before saturation effects occur. For example, the hydrogen concentration for the upper profile in figure 4 corresponds to about ten percent.

It is particularly interesting to look at the release of the hydrogen from traps in order to determine the binding of the hydrogen to these traps. The profiles are reduced uniformly in depth upon annealing, indicating that the hydrogen is released from traps and then diffuses rapidly: Diffusion-controlled processes would lead to a broadening of the profiles. We also conclude that in the release process the trap centers are not annihilated, because there is no loss of trapping efficiency if a predamaged sample is annealed to temperatures sufficient to release the hydrogen and then at lower temperatures is reinjected with hydrogen. The broad temperature dependence of the detrapping indicates the process involves a distribution of trap energies, and the high temperatures (about 200°C) for release imply activation energies of the order of 1.5 eV. This value is surprisingly high compared with other studies of hydrogen trapping. For example, for cold-worked steels or for dislocations in niobium, typical trapping energies of 0.1 to 0.4 eV are observed. Such energetic damage trapping for hydrogen does not appear to be a universal phenomenon for the metals; however, it is also found for ion damage in niobium, where the solubilities and diffusivities for hydrogen are much greater. Open vacancy-rich structures have been suggested as the cause of the trapping, but the effect is far from understood.

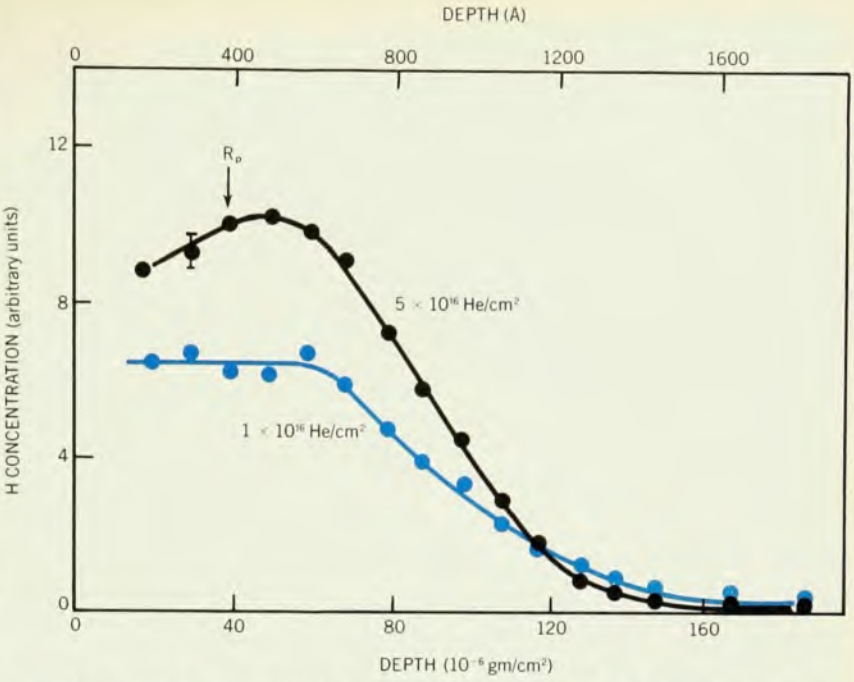

Trapped-hydrogen profiles for molybdenum predamaged with helium. The depth profile for the Mo with more predamage (upper curve) shows more retention of the hydrogen before saturation occurs; the maximum here corresponds to about 10 atomic percent. Before saturation, nearly 100% trapping is observed. From reference 6. Figure 4

Bubbles and blisters

At high hydrogen concentrations precipitation can occur either into a hydride phase or into gas bubbles. If gas bubbles form, deformation of the surface may occur as more hydrogen is added. The occurrence of gas bubbles and blisters is a widely observed phenomenon for helium implantation in metals, and it can also occur for hydrogen implants for sufficiently high hydrogen accumulations. From information based largely on helium studies, gas bubbles are believed to begin to form at room temperature and below for concentrations greater than about 4%, and blistering or other modes of surface deformation occurs at concentrations of about 30 to 40%.

An example of a blistered surface for deuterium implantation in tungsten is seen in figure 5. The concentration here is 1×10^{18}D per cm², implanted at 30 keV. Some of the blister lids have flaked (fractured) from the surface. The blister size distribution shown in the micrograph has a most probable diameter between 1 and 2 microns.

In an attempt to understand these phenomena better, the integrated stress that builds up in these layers during implantation has recently been measured.[7] A "gas-pressure" model to describe the development of the blister lids has been widely held to explain these phenomena. Recently, however, as more data accumulate, this model has become less satisfactory, so the stress that is built up in the implanted layers was examined by the bending of a cantilevered beam. This study has led to an "elastic instability model"[7] for blistering. One success of this model has been to describe reported data on the blister-lid diameter and blister-lid thickness at relatively low temperatures. Different behavior, such as large-area flaking, can occur at higher temperatures.

In this model

$$t = d^{2/3}[(1 - p^2)S_m/2E]^{1/3}$$

where t is the most probable blister-lid thickness, d is the most probable diameter, p is Poisson's ratio, E is Young's modulus, and S_m is the maximum depth-integrated stress in the implanted layer before blistering occurs. The maximum depth-integrated stress has been observed to depend approximately linearly on the yield stress of the material, and this correlation has allowed comparison of the predicted functional dependence and magnitude of d and t with no free parameters on the one hand, with the

Nuclear techniques for hydrogen detection and depth profiling

Technique	Example	Major advantage	Major disadvantage
Resonant reactions	$H^1(F^{19},\alpha\gamma)O^{16}$	Good depth resolution	Requires higher beam energies
Nonresonant reactions	$H^2(He^3,p)He^4$	High sensitivity	Long analysis times for depth profiles
Elastic scattering	$H^2(p,p)H^2$	Versatility	Low sensitivity
Elastic recoils	$H^1(Cl^{35},Cl^{35})H^1$	High sensitivity	Requires thin films or glancing angles

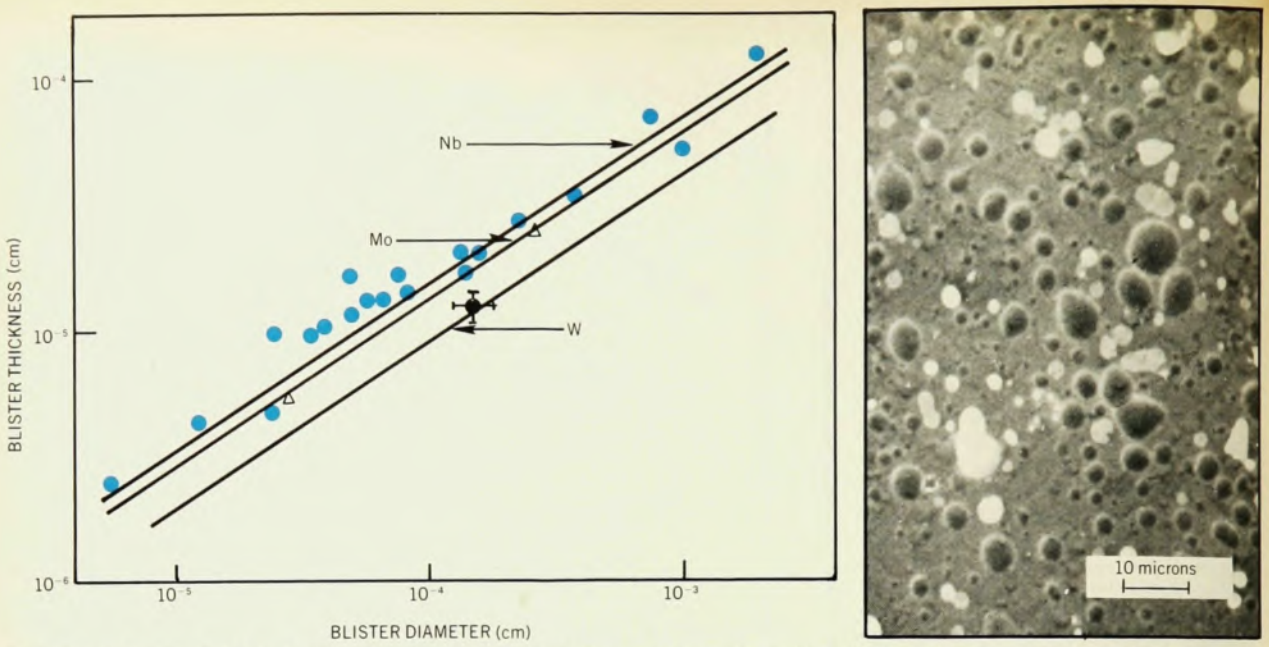

Blistering of metal surfaces can occur at high hydrogen-isotope concentrations. The electron micrograph shows a tungsten surface after implantation with 1×10^{18} per cm^2 of 30-keV deuterium. White areas show where some of the blister lids have flaked from the surface. Plots of approximate blister thickness (t) versus diameter (d), for studies of He in Nb (color dots), He in Mo (triangles) and H^2 in W (black dot) appear to agree with an elastic-instability model shown here by the three black lines for Nb, Mo and W. From reference 7. Figure 5

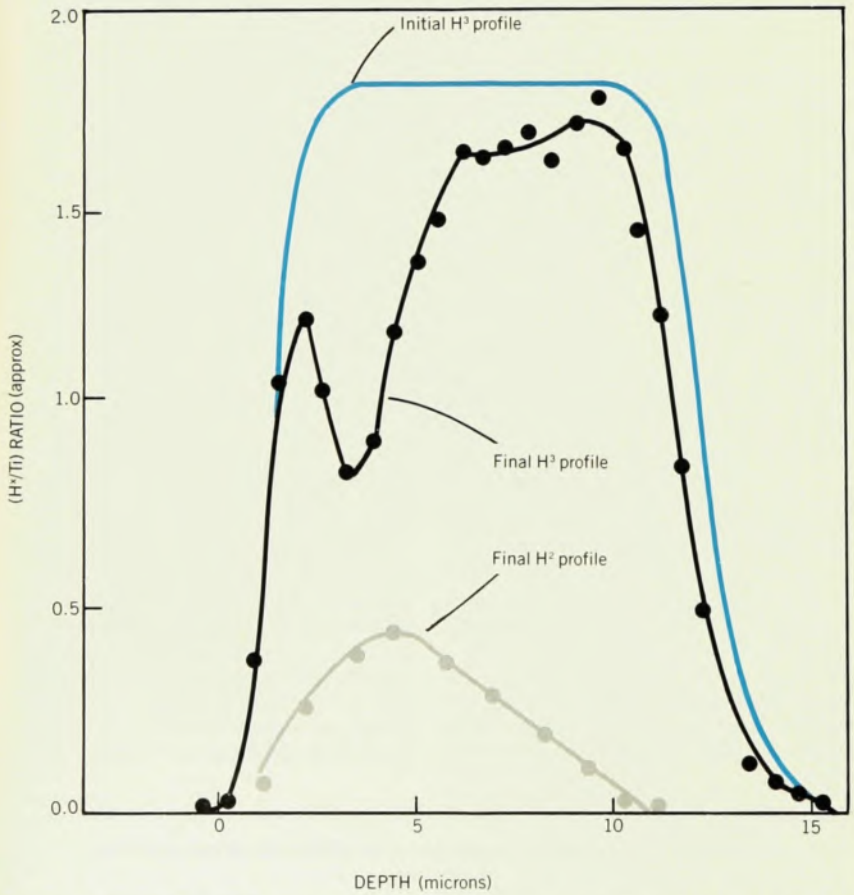

Depth profiles of H^3 and H^2 in neutron-production targets help explain why these tritiated titanium targets degrade after about 100 hours. They are bombarded with 400-keV H^2 to produce 14-MeV neutrons used in fusion-energy simulation studies. An H^3 profile before (color) and after (black) degradation shows that the dip in the H^3 concentration is near the point of maximum H^2 concentration (gray). a neutron time-of-flight analysis was used here. From reference 8. Figure 6

many experimental observations available on the other. An example in figure 5 of preliminary results for helium implants in niobium and molybdenum and for deuterium-implanted tungsten suggests a favorable agreement for this description.

The blistering phenomena appear to be basically mechanical failure processes on a microscopic scale, and the recent results tend to support the idea that the extremely high stresses parallel to the surface are the primary cause of blistering. Presumably these stresses are a result of the swelling caused by the gas bubbles. Although there is still considerable controversy among researchers on the mechanisms, progress is being made on understanding these complex phenomena that border one limit of the high-concentration regime.

Films and corrosion

Another interesting limiting case is the formation of hydride phases at very high concentration. A fascinating example[3] is the tritium depth-profile study of the degradation of neutron-production targets.[8] Tritiated titanium targets are bombarded with 400-keV deuterons, producing 14-MeV neutrons to simulate environments for fusion-energy materials studies. However, after 100 hours of operation, the neutron output for the targets drops to about 70 to 80% of the initial output. The $H^3(p,n)$ nuclear reaction (nonresonant technique) was used for the depth profile of tritium; the energy of the emitted neutrons was analyzed with time-of-flight techniques. In this method the probing depth is in excess of 10 mi-

Low prices. Good selection. That's Granville-Phillips.

BAYARD-ALPERT IONIZATION GAUGE TUBE PRICE COMPARISON

A. 3/4 in. Pyrex, Dual Tungsten Filments
B. 3/4 in. Kovar, Dual Tungsten Filaments
C. 3/4 in. Pyrex, Iridium Filament
D. 3/4 in. Kovar, Iridium Filament
E. 1 in. Kovar, Iridium Filament
F. 2-3/4 in. o.d. Flange on 1 in. Kovar, Iridium Filament

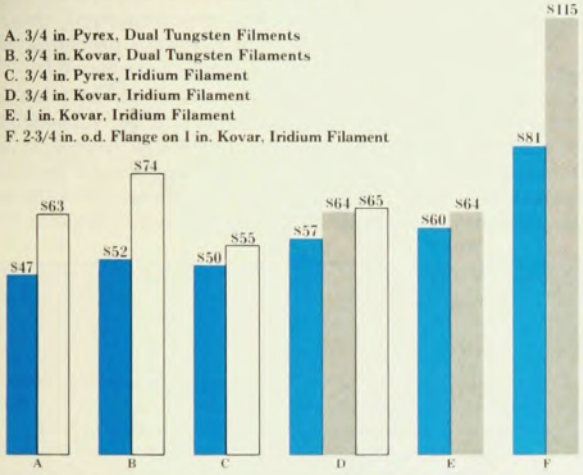

CUSEAL*-CONFLAT® FLANGE PRICE COMPARISON

GPC February 1977 Prices
VARIAN July 1977 Prices
VEECO 1977 Catalog Prices (Received March, 1977)

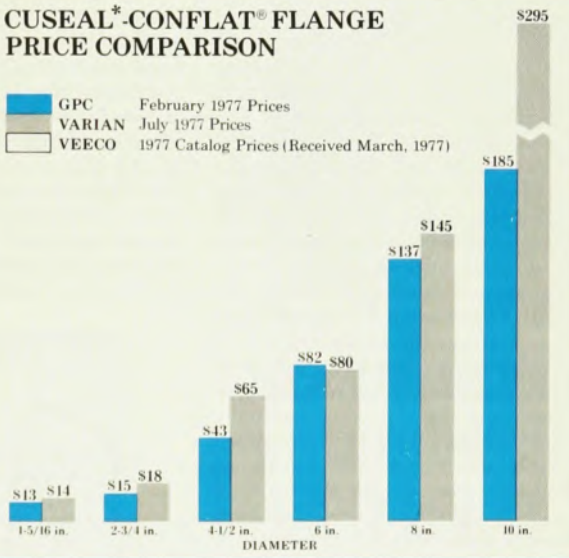

Granville-Phillips has the industry's widest selection of low priced ionization gauge controllers. Both Bayard-Alpert and Schulz-Phelps models in industrial and UHV designs. Readout only or with process control, Pirani gauge tube or thermocouple gauge tube options. And an extensive choice of low priced ionization gauge tubes for applications ranging from 10^{-11} Torr to 1 Torr.

Pressure measurement is a primary area for Granville-Phillips. Not just a sideline in a something-for-everybody catalog.

Our prices are low. 83% of our Cu-Seal flanges are priced lower than similar Conflat flanges. Most CuSeal prices declined in early 1977 due to increased productivity. Most Conflat prices have increased twice in 1977.

We don't sacrifice quality for price. We use vacuum processed 304 stainless steel exclusively in our flanges. It costs us 33% more than ordinary bar stock but greatly reduces the risk of porosity and virtual leaks. We manufacture every flange in-house to control the entire process and make nine inspections between raw material purchase and finished flange.

We concentrate on making a few very good product lines. Not a lot of average ones. That means we can concentrate on giving you lower prices. Better selection. Better quality. That's better value. It's yours when you buy from Granville-Phillips.

*CuSeal flanges are manufactured to geometries licensed by Varian. Conflat is a registered trademark of Varian Associates.

GRANVILLE-PHILLIPS
5675 EAST ARAPAHOE AVENUE
BOULDER, COLORADO 80303, U.S.A.
PHONE 303/443-7660 • TELEX 045-791

Where you buy with confidence.

Circle No. 24 on Reader Service Card

crons, and the resolution varies with depth from about 0.3 to 1.1 microns, limited primarily by energy straggling of the incident protons. A depth profile of the tritium before and after film degradation is seen in figure 6, along with the profile of the collected deuterium obtained from the $H^2(d,n)$ reaction. The dip in the tritium concentration occurs at a depth near that where the deuterium comes to rest. The total incident deuterium fluence was enough to replace all the tritium three times, whereas only about 15% of the tritium was lost and about the same amount of deuterium was collected. The theoretical yield from such a profile is calculable, and the observed degradation is in good agreement with that number.

At these very high hydrogen isotope concentrations for hydrides, the elastic scattering of protons can also be used for deuterium and tritium profiling. One example is the 2.5-MeV proton-scattering analysis of thick and thin tritium-deuteride targets.[9] From the energy edges, corresponding to the front and rear film surfaces, we can obtain the proton energy loss in going through the film and determine the depth distribution of the deuterium. At the same time other information, such as the implanted-helium depth distribution, the surface carbon and oxygen contamination, the titanium layer thickness and the thickness nonuniformity, is obtained. Thus the versatility of this technique is its main advantage. Elastic scattering is also applicable to thick targets, but the higher backgrounds reduce the sensitivity, which in all cases tends to limit studies to systems with the order of 1% or more deuterium or tritium. Sufficient sensitivity for the proton elastic-scattering method arises from the 10^2 to 10^3 enhancement in the cross section for deuterium and tritium over Rutherford values, whereas little or no nuclear-scattering enhancement is obtained for the heavier substrate atoms at these proton energies of 2 to 3 MeV.[9,10]

Metallurgy has not received nearly enough attention by nuclear-reaction techniques. One example from the study of hydrogen profiles in an aluminum alloy after stress-corrosion exposure[11] is seen in figure 7. This high-temper alloy is particularly susceptible to stress-corrosion cracking, possibly caused by hydrogen embrittlement. In this example the hydrogen concentration has been measured in the first few microns by means of the $H^1(Li^7,\gamma)$ reaction in a resonance technique. The profiles were obtained after exposure to a 3.5% aqueous chloride solution and without exposure, both while under 50 ksi applied stress. A large accumulation of hydrogen is observed in the exposed surface compared with the less than 140 atomic parts per million hydrogen level in the unexposed surface. The appreciable concentration penetration is probably due to the very high concentration regions for penetrating cracks, which may be where the stress-corrosion cracking initiates. The hydrogen concentration is strongly stress dependent. The amount of hydrogen increases with stress until appreciable plastic yielding occurs (70% of the yield stress); from this point on there is reduced hydrogen penetration. In another recent metallurgical application of ion beam techniques, the microhardness of electrodeposited gold (for use as sliding electrical contacts) has been correlated with the presence of high hydrogen concentrations, and not with the presence of cobalt and nickel as had been previously believed.[12]

We end with an example of antiquities dating with ion beam techniques. Atmospheric hydrogen interacts with many glasses to form a hydrated layer. This interaction is a diffusion-limited process, so that the time since the surface was first exposed (for example, by chipping to make an obsidian artifact) can be related to the thickness of the hydrated layer. The diffusion coefficients are such that a layer of two microns for obsidian corresponds to about 1000 years. Optical methods of determining thickness of hydration for obsidian are standard, but greater resolution and accuracy can be obtained by profiling the hydrogen in the layer with nuclear reaction techniques. By artifact dating from different regions of the world and by experiment we now know that the effective diffusion coefficient obeys a normal thermally activated behavior:[13] that is, samples from hot regions form hydrated layers more quickly than do samples from cold regions.

In recent $H^1(N^{15},\alpha\gamma)$ resonant profiling measurements[14] these ideas have been extended to observations of manmade glass. In figure 8 we see both step and sloping profiles, with a glass doorknob and other more decorative glass giving the sloping profiles. The preliminary study has indicated that this process also appears to be diffusion limited.

Research on the behavior of hydrogen in materials is very important, then, to many current materials problems, particularly in energy-related studies. The techniques for hydrogen detection and profiling are quite simple. Although the methods are fairly well developed and understood, their application to hydrogen-materials studies are quite exciting and are only beginning to blossom forth

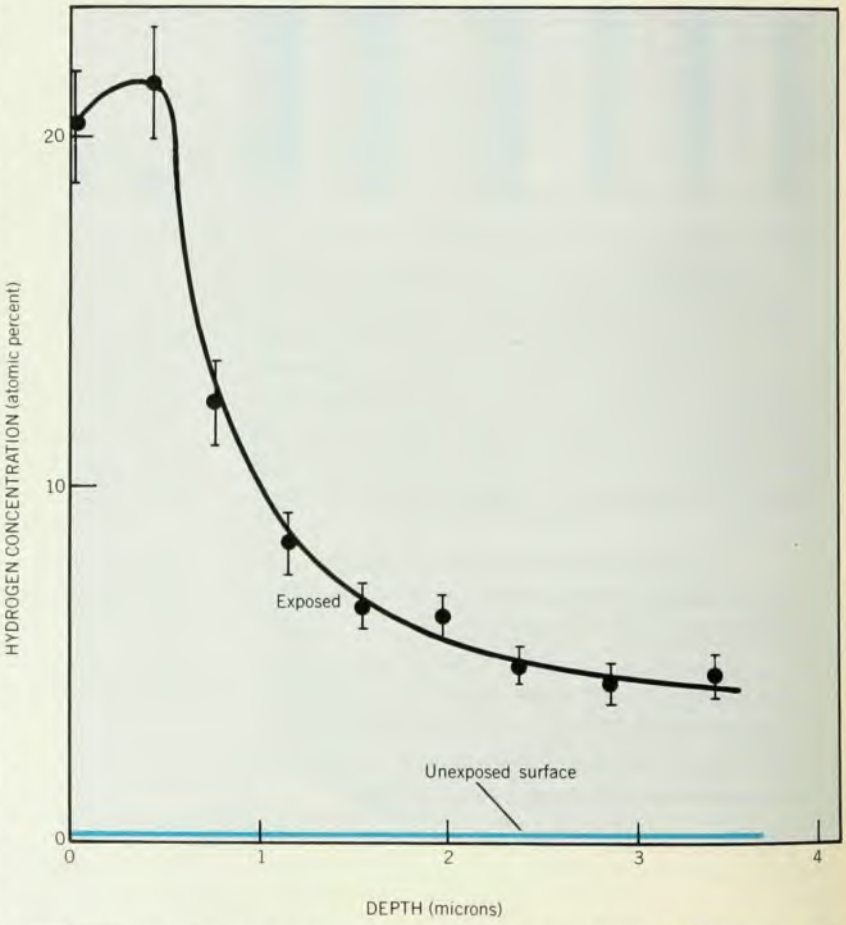

Stress corrosion simulation is seen to affect the hydrogen depth profile in 7075-T651 Al alloy. The hydrogen profiles (resonant reaction method) were done at 50 ksi applied stress both with (black) and without (color) exposure to a 3.5% aqueous-chloride solution with a pH of 2. The exposed surface has a much higher H concentration. Such studies help build models of stress-corrosion cracking. From reference 11. Figure 7

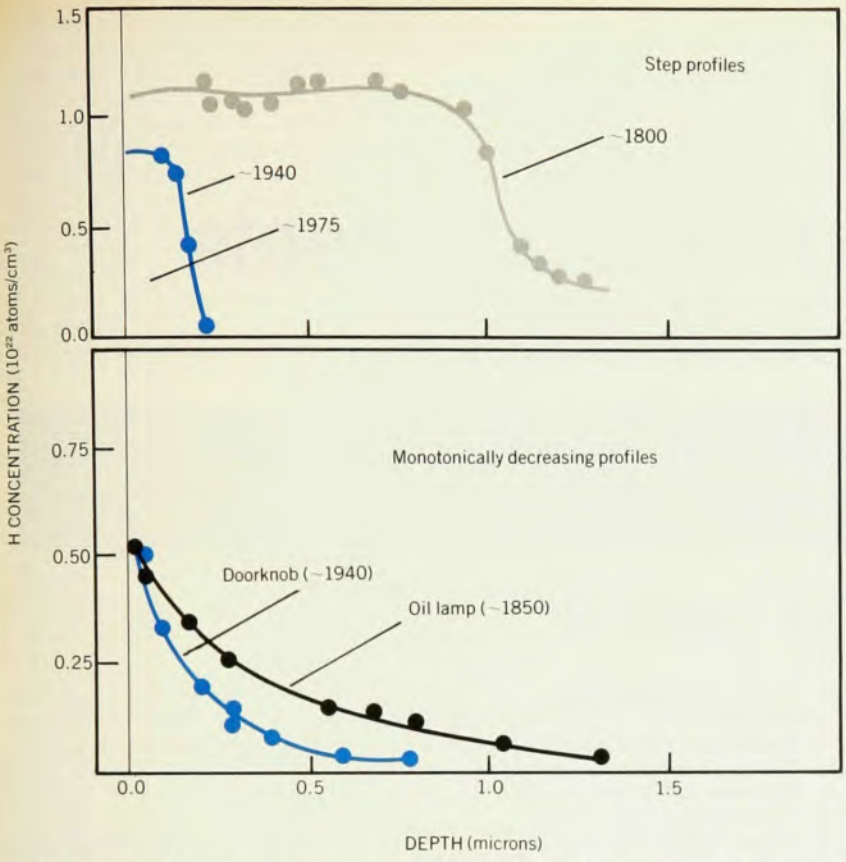

Hydration profiles of manmade glass samples. These hydrogen profiles, obtained with the resonant reaction method, demonstrate the dating of antiquities. The sloping profiles are more prevalent for decorative glasses, whereas the step profiles are commonly observed for plain glass. The thickness of the hydrated layer is a measure of age, and preliminary studies suggest that the hydration process is diffusion limited here as well as in obsidian artifacts. From reference 14. Figure 8

in the ways described in this article.

* * *

This article is adapted from a paper presented at the April 1977 meeting of The American Physical Society in Washington, D.C. I thank Fred Vook for his valuable comments and the Energy Research and Development Administration for its support.

References

1. J. Bottiger, S. T. Picraux, N. Rud, in *Ion Beam Surface Layer Analysis* (O. Meyer, G. Linker, F. Kappeler, eds), Plenum Press, N.Y. (1976), page 811; see also other articles in these conference proceedings.
2. *Proceedings* of the Third International Conference on Ion Beam Analysis, Washington, D.C., June 1977, (to be published in Nucl. Inst. and Methods).
3. D. A. Leich, T. A. Tombrello, Nucl. Inst. and Methods **108,** 67 (1973).
4. S. T. Picraux, in *New Uses of Low Energy Accelerators* (J. F. Ziegler, ed), Plenum Press, N.Y. (1975) page 229; F. L. Vook, S. T. Picraux, in *Advances in Chemistry Series No. 158: Radiation Effects on Solid Surfaces* (M. Kaminsky, ed), American Chemical Society (1976) page 308.
5. S. T. Picraux in reference 1, page 527.
6. S. T. Picraux, J. Bøttiger, N. Rud, J. Nucl. Materials **63,** 110 (1976).
7. E. P. EerNisse, S. T. Picraux, J. Appl. Phys. **48,** 9 (1977).
8. J. C. Davis, J. D. Anderson, J. Vac. Sci. Technol. **12,** 358 (1975).
9. R. S. Blewer in reference 1, page 185.
10. R. A. Langley in reference 1, page 201.
11. P. N. Adler, G. M. Padawer, E. A. Kamykowski, *Proceedings* of the 1974 Tri-Service Corrosion of Military Equipment Conference, AFML-TR-75-42, vol. II, page 25, WPAFB, Ohio.
12. G. J. Clark, C. W. White, D. D. Allred, B. R. Appleton, I. S. T. Tsong, F. B. Koch, C. W. Magee, D. E. Carlson, to be published in reference 2.
13. I. Friedman, R. L. Smith, W. D. Long, Geological Soc. Amer. Bulletin **77,** 323 (1966).
14. W. A. Lanford, Science **196,** 975 (1977).
15. M. H. Brodsky, M. A. Frisch, F. J. Ziegler, W. A. Lanford, Appl. Phys. Lett. **30,** 561 (1977).
16. P. N. Adler, E. A. Kamykowski, G. M. Padawer, *Hydrogen in Metals* (I. M. Bernstein, A. W. Thompson, eds) American Society for Metals (1974) page 623.
17. W. A. Lanford, R. C. Dynes, J. M. Poate, J. M. Rowell, T. H. Schmidt, to be published.
18. W. A. Lanford, to be published in reference 2; W. A. Lanford, R. Golub, submitted to Phys. Rev. Lett. □